Orienting Actin Filaments for Directional Motility of Processive Myosin Motors

ARTICLE *in* NANO LETTERS · DECEMBER 2012

Impact Factor: 13.59 · DOI: 10.1021/nl303500k · Source: PubMed

4 AUTHORS, INCLUDING:

Jinzhou Yuan
University of Pennsylvania
12 PUBLICATIONS **50** CITATIONS
SEE PROFILE

Anand Pillarisetti
University of Maryland, College Park
19 PUBLICATIONS **346** CITATIONS
SEE PROFILE

Haim H Bau
University of Pennsylvania
259 PUBLICATIONS **6,421** CITATIONS
SEE PROFILE

NANO LETTERS

Letter

pubs.acs.org/NanoLett

Orienting Actin Filaments for Directional Motility of Processive Myosin Motors

Jinzhou Yuan,[†] Anand Pillarisetti,[†] Yale E. Goldman,[‡,§] and Haim H. Bau*[,†]

[†]Department of Mechanical Engineering and Applied Mechanics, [‡]Department of Physiology, and [§]Pennsylvania Muscle Institute, School of Medicine, University of Pennsylvania, Philadelphia, Pennsylvania 19104, United States

Supporting Information

ABSTRACT: To utilize molecular motors in manmade systems, it is necessary to control the motors' motion. We describe a technique to orient actin filaments so that their barbed ends point in the same direction, enabling same-type motors to travel unidirectionally. Myosin-V and myosin-VI were observed to travel, respectively, toward and away from the filaments' barbed ends. When both motors were present, they occasionally passed each other while "walking" in opposite directions along single actin filaments.

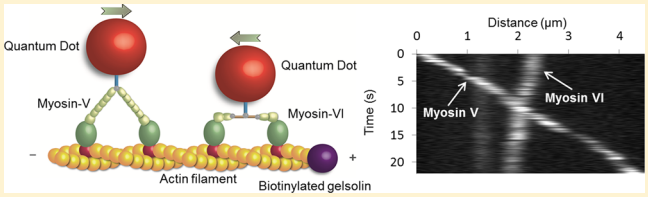

KEYWORDS: *Actin, myosin, molecular motor, shuttle, transport, device*

In recent years, there have been growing efforts to engineer miniaturized devices using purified macromolecules as the elementary building blocks. These efforts are driven by the desire to both deepen our understanding of biology—"build life to understand it"[1]—and develop devices that either utilize biological machines as components or use biology to guide engineering design.[2−4] Molecular motors drive a myriad of processes in cells such as targeted delivery of vesicles; localization of organelles, mRNAs, and chromosomes; modulation of mechanical properties; and spindle dynamics during mitosis.[5] We focus here on processive molecular motors such as myosin V and myosin VI that travel along tracks such as actin filaments (F-actin). The F-actin has structural polarity. One end of the filament is known as the barbed (plus) end and the other as the pointed (minus) end. Most actin-based motors, that is, myosin V, travel in the direction of the barbed end, but another motor, myosin VI, travels in the opposite direction, toward the pointed end. To utilize molecular motors as cargo-carrying shuttles in manmade systems, it is necessary to control their directions of motion.[2,3]

Inspired by nature, various researchers have attempted to utilize processive motors as actuators in vitro. Generally, in vitro assays are classified into gliding assays and processive motility assays. In gliding assays, the protein motors are adsorbed to a substrate, and their tracks (i.e., microtubules or actin filaments) are propelled by the motors. In processive motility assays, the tracks are immobilized to a surface, and the protein motors "walk" along the tracks. In either case, it is desirable to control the polarity (direction) of the tracks.[6] In gliding assays, control of directionality has been achieved with micro patterned structures,[7−16] electric fields,[17−19] and/or shear flows.[20−24] To control the directionality of the tracks in processive motility assays, researchers have used specific proteins that bind selectively to a specific end of the microtubule[25,26] or actin filament[27−29] to anchor the polymer to a surface at that particular end. Then, the shear flow of the bathing solution was used to orient the tracks. The challenge is, however, to immobilize the oriented tracks on the surface in a polarized fashion without compromising the motors' motility. Although methods for oriented assembly of actin filaments on surfaces[27−29] and motor motility along the oriented filaments[28] have been previously described, there are no reports of orienting and immobilizing actin filaments with predetermined polarization and maintaining the polarization after the orienting field was removed. These features are crucial for devices that utilize molecular motors as shuttles.

In this Letter, we describe a method, dubbed the polarized assay, to orient and immobilize actin filaments onto a surface without inhibiting molecular motors' motility. The velocity, run length, run frequency, and direction of motion of the motors in the polarized assay were critically compared with similar metrics in conventional, nonpolarized assays. Simultaneous bidirectional cargo transport was achieved by deploying both myosin V and myosin VI motors, which "walk" in opposite directions along actin filaments. Myosin V and VI were observed, for the first time, to pass each other while walking in opposite directions along a single actin filament.

Briefly, the actin filaments were capped at their barbed (plus) ends with biotinylated gelsolin, bound to streptavidin immobilized on the glass microscope slide, leading to (+) end attachment. Then, the filaments were flattened against the glass by flow of a medium containing poly-L-lysine, which kept the filaments attached to the surface after the flow ceased. The experimental apparatus consisted of a 140 μm tall flow cell

Received: September 19, 2012
Revised: December 7, 2012
Published: December 14, 2012

   dx.doi.org/10.1021/nl303500k | *Nano Lett.* 2013, 13, 79−84

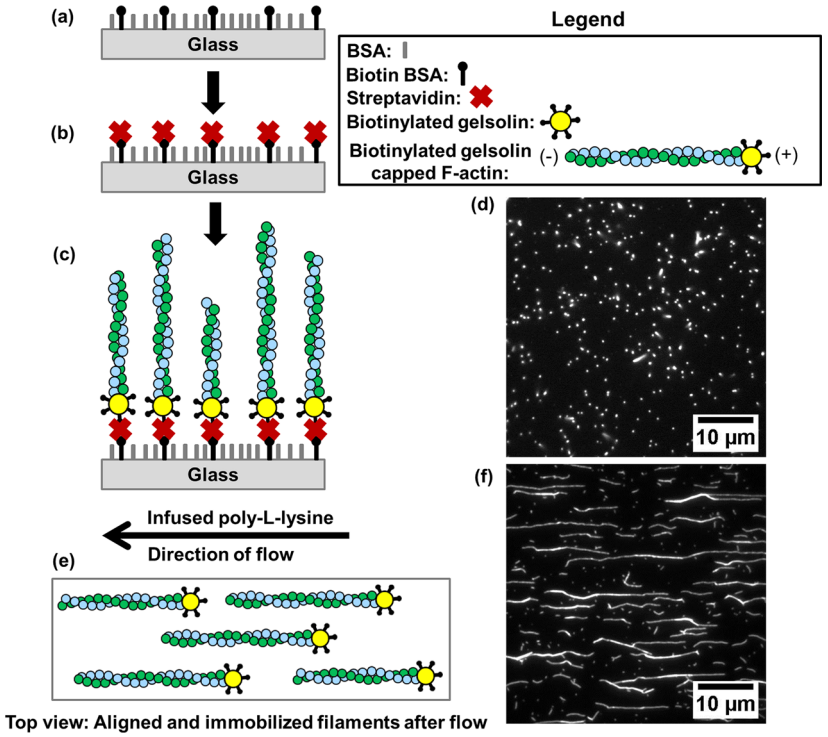

Figure 1. Polarized assay. BSA and biotinylated BSA-coated glass surface (a). Streptavidin bound to the immobilized, biotinylated BSA (b). Plus *end-on* attached actin filament: schematic depiction (c) and experimental photograph (d). *Side-on* attached actin filament: schematic depiction (e) and experimental photograph (f).

sandwiched between a glass slide (Fisher Scientific, 125495) and a coverslip (Fisher Scientific, 1254587). The flow was induced in the device by wicking the cell solution with filter papers. Figure 1 depicts the various steps involved in the assay. The inner surface of the flow cell was coated with a mixture of bovine serum albumin (BSA; Sigma, A0281) and biotinylated BSA (Sigma, A8549) at the ratio of 9:1 (Figure 1a). A solution of streptavidin (Sigma, S4762) was then transfused through the flow cell. The streptavidin bonded to the biotinylated BSA (Figure 1b), and any unbound streptavidin was washed away. Subsequently, actin filaments, capped with biotinylated gelsolin at their barbed ends and labeled with rhodamine phalloidin, were transfused through the flow cell and bonded to the immobilized streptavidin with the filaments' axes pointing away from the surface (Figure 1c and d). We refer to this configuration as *end-on attachment*. The nearly vertical orientation of the actin filaments was likely caused by electrostatic repulsion between the negatively charged filaments and the negatively charged BSA-coated slide. Since gelsolin binds preferentially to the actin's barbed end,[30] the filaments attached to the surface at their barbed ends, while their minus (pointed) ends were away from the surface. Figure 1d is a total internal reflection fluorescence (TIRF) microscopy image of the fluorescent-labeled actin filaments attached end-on to the surface. Each bright dot in the photograph corresponds to an actin filament's barbed end. The density of the actin filaments in the polarized assay was $(1.4 \pm 0.5) \times 10^5$ filaments/mm^2. When the experiment was repeated with actin filaments that were not functionalized with biotinylated gelsolin (Figure S1 in the Supporting Information), only $(7.6 \pm 2.6) \times 10^2$ filaments/mm^2 were observed to (nonspecifically) attach to the streptavidin-coated surface. This suggests that, in the polarized assay, over 99% of the filaments were specifically bound at their barbed ends via the biotinylated gelsolin.

The flow cell was then subjected to the flow of a solution containing poly-L-lysine (MP Biomedicals, 0871120G) at a concentration of 50 μg/mL that flattened the actin filaments down onto the surface (Figure 1e and f). The poly-L-lysine solution flipped the electric charge of the surface from negative to positive, inducing an electrostatic force that retained the filaments firmly attached to the surface after the cessation of the flow. We refer to this attachment step as *side-on attachment* (Movie S1 of the Supporting Information). When the flow was directed from right to left, the side-on attachment resulted in actin filaments flattened onto the surface with their plus ends pointing upstream, to the right (Figure 1f). In the polarized assay, the filament surface coverage was 160 ± 90 mm actin length per mm^2 of surface area. We experimented with various poly-L-lysine concentrations. The concentration of 50 μg/mL is the minimum needed for the firm attachment of the actin filaments to the surface. At poly-L-lysine concentrations below 50 μg/mL, portions of the filaments were detached from the surface and subject to thermal fluctuations, which interfered with motility studies.

To verify the polarity of the immobilized actin filaments, we infused the flow cell with a solution containing myosin V motors attached to ~20 nm diameter quantum dots (Invitrogen, Q10161MP, QD 655 nm). In the presence of 10 μM MgATP and 3.3 nM myosin V motor-coated quantum dots (labeling ratio: 1.5 motors/1 quantum dot), most (95% ± 1%, n = 774) of the myosin V motor-coated quantum dots traveled from left to right (Movie S2 of the Supporting Information). Since myosin V motors only travel toward the barbed ends, the experiment confirmed that the actin filaments were, indeed, oriented with their plus ends facing to the right.

dx.doi.org/10.1021/nl303500k | *Nano Lett.* 2013, 13, 79−84

As a control experiment, we used a nonpolarized assay, in which biotinylated, rhodamine phalloidin labeled actin filaments were aligned solely by fluid flow and anchored to the streptavidin-coated glass substrate by the biotin incorporated in the F-actin. In the nonpolarized assay, without any initial specific end-on attachment, the actin filaments were orientated with their barbed ends pointing randomly either to the left or the right and the myosin V motor-coated quantum dots traveling in both directions in nearly equal proportions.

The alignment of filaments in the polarized and nonpolarized assays was quantified by measuring the angular distributions of the total of actin filaments' lengths (Figure 2a and b) and the distances traveled by myosin V motor-coated quantum dots (Figure 2c and d). In Figure 2, the angle $\theta = \pi$ corresponds to the direction of the flow used in the *side-on* attachment. The polarity of each actin filament was determined by the direction of motion of the myosin V motor-coated quantum dots. The length of actin filaments as a function of the angle θ was measured with the aid of ImageJ software. In both assays, most of the filaments were parallel to the flow direction. We use $L(\theta)$ to denote the sum of the lengths of the filaments' segments oriented in the $\theta \pm \Delta\theta/2$ direction. The experimentally determined probability density function of the sum of the filaments' lengths oriented in the $\theta \pm \Delta\theta/2$ direction, $L(\theta)/(L_T\Delta\theta)$, is depicted as a function of the angle θ when the assay is nonpolarized (Figure 2a, bars) and when the assay is polarized (Figure 2b, bars). In the above, L_T is the total length of the filaments and $\Delta\theta = 5°$. The majority of the actin filaments in the polarized assay are oriented with their plus ends pointing to the right (Figure 2b), whereas there is no such preference in the nonpolarized assay (Figure 2a). The probability density function of the actin filaments in the polarized assay can be approximated with the Gaussian distribution

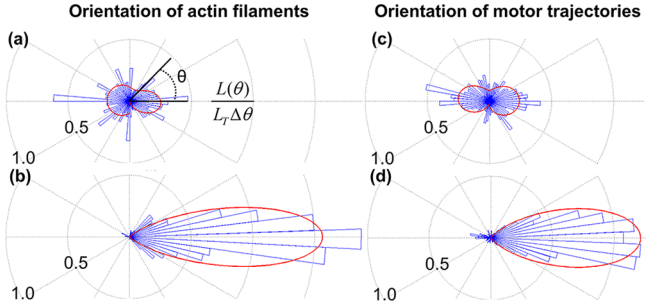

Figure 2. Probability density function of the sum of the filaments' lengths as a function of orientation θ in the nonpolarized assay (a) and the polarized assay (b). The probability density function of the distance traveled by myosin V motors as a function of orientation θ in the nonpolarized assay (c) and the polarized assay (d).

$$f(\theta) = \frac{1}{\sigma\sqrt{2\pi}} e^{-1/2\left(\frac{\theta}{\sigma}\right)^2} \quad (1)$$

where $\sigma = 0.25$, $R^2 = 0.88$, and both θ and σ are expressed in radians (red line in Figure 2b). In contrast, the probability density function of the actin filaments in the nonpolarized assay can be approximated with the bimodal Gaussian distribution

$$f(\theta) = \frac{A}{\sigma_1\sqrt{2\pi}} e^{-1/2\left(\frac{\theta-\theta_1}{\sigma_1}\right)^2} + \frac{1-A}{\sigma_2\sqrt{2\pi}} e^{-1/2\left(\frac{\theta-\theta_2}{\sigma_2}\right)^2} \quad (2)$$

where $A = 0.33$, $\theta_1 = -0.11$, $\theta_2 = 3.00$, $\sigma_1 = 0.56$, $\sigma_2 = 1.45$, $R^2 = 0.22$, and both θ and σ are expressed in radians (red line in Figure 2a). The Ashman's test[31] is often used to examine whether the means of the two distributions are sufficiently separated to constitute a bimodal distribution. In our case,

$$D = \frac{\sqrt{2}|\theta_1 - \theta_2|}{\sqrt{\sigma_1^2 + \sigma_2^2}} = 2.8 \quad (3)$$

$D > 2$ suggests a bimodal distribution.

The trajectories of motors were recorded with 100 ms exposure time at 10 frames per second and quantified using the Fluorescence Image Evaluation Software for Tracking and Analysis (FIESTA) program.[32] Since we were primarily interested in the directionality of the actin filaments, periods of low or zero motor velocity were filtered out by a custom algorithm that averaged groups of successive positions within a radius of 50 nm (Figure S2 of the Supporting Information). In the polarized assay, about 95% ± 1% ($n = 774$) of the myosin V motor-coated quantum dots traveled to the right ($-\pi/2 < \theta < \pi/2$) compared with only about 58% ± 4% ($n = 159$) in the nonpolarized assay (Figure 2c and d). We use $N_D(\theta)$ to denote the fraction of the total distance traveled by myosin V motor-coated quantum dots in the direction $\theta \pm \Delta\theta/2$ ($\Delta\theta = 5°$) as a function of the angle θ. Figures 2c and d, respectively, depict the experimental probability density function $N_D(\theta)/\Delta\theta$ as a function of θ (bars) in the nonpolarized assay and the polarized assay. In the polarized assay, we can approximate the probability density function of the distance traveled by myosin V motor-coated quantum dots with the Gaussian distribution function (eq 1) with $\sigma = 0.33$, $R^2 = 0.95$, and both θ and σ are expressed in radians (red line in Figure 2d). In contrast, the probability density function of the distance traveled by myosin V motor-coated quantum dots in the nonpolarized assay can be approximated with the bimodal Gaussian distribution (eq 2), where $A = 0.54$, $\theta_1 = 0.02$, $\theta_2 = 3.02$, $\sigma_1 = 0.89$, $\sigma_2 = 0.72$, $R^2 = 0.40$, and both θ and σ are expressed in radians (red line in Figure 2c). According to Ashman's test $D = 3.69$, indicating bimodal distribution.

The net distance that the motors moved to the right (in the $\theta = 0$ direction) was determined by summing up the projections of all motor trajectories, regardless of the direction of motion, onto the $\theta = 0$ axis. The transport efficiency is defined as the ratio between the net distance that the motors traveled to the right and the total distance that the motors traveled regardless of direction. In the polarized assay, the transport efficiency was approximately 78% ± 6%, whereas in the nonpolarized assay, the transport efficiency was only 10% ± 12%. The transport efficiency of the polarized assay falls short of the desired 100%, perhaps due to imperfect surface blocking that resulted in nonspecific attachment of a few actin filaments during the initial end-on attachment step and, perhaps even more so, during the side-on attachment. In the latter case, it is possible that a few filaments detached or broke during the application of the aligning shear flow and then reattached nonspecifically.

To quantify the motility of the molecular motors, we measured the myosin V motor-coated quantum dots' speed, run length, and run frequency in the polarized and nonpolarized assays. Figures 3a and b depict the histograms of the myosin V motor-coated quantum dots' speed and run-length, respectively. The average speeds and run lengths of myosin V motor-coated quantum dots were 174 ± 50 nm/s ($n = 91$) and 1334 ± 884 nm ($n = 91$) in the nonpolarized assay (red) and 129 ± 51 nm/

dx.doi.org/10.1021/nl303500k | Nano Lett. 2013, 13, 79−84

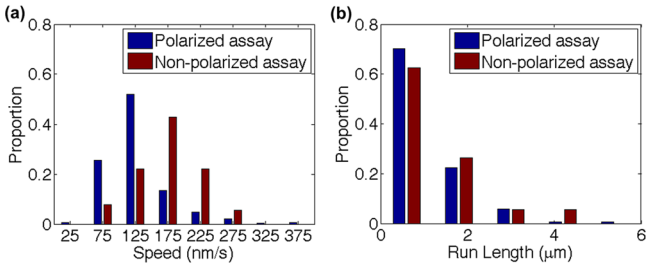

Figure 3. Proportion of myosin V motors as a function of velocity (a) and run length (b) for the nonpolarized assay (red, n = 91) and a polarized assay (blue, n = 273).

s (n = 273) and 1104 ± 823 nm (n = 273) in the polarized assay (blue). In the above, ± X corresponds to a standard deviation. In the polarized assay, the average motors' velocity and run length were slightly less than in the nonpolarized assay (p < 0.05).

The run frequency is defined as the number of active motor-coated quantum dots per minute per 10 μm of filament length. The run frequency serves to assess the rate of processive runs of motor-coated quantum dots on the filament. The run frequencies were, respectively, 2.6 ± 0.3 and 2.0 ± 0.7 motor-coated quantum dots per minute per 10 μm of filament length in the nonpolarized and the polarized assays when both assays had the same concentrations of myosin V motor-coated quantum dots (3.3 nM) with the same motor-quantum dot labeling ratio (1.5:1).

In summary, the average speed, average run length, and run frequency in the polarized assay were, respectively, smaller by approximately 26%, 17%, and 23% than in the nonpolarized assay. These small reductions in average speed, run length, and run frequency were possibly caused by electrostatic interactions between the negatively charged myosin V motors and the positively charged poly-L-lysine-modified surface and by poly-L-lysine adsorbing to the actin filaments and presenting obstacles in the molecular motors' paths.[33]

The directionality of the actin filaments was also investigated by infusing the flow cell with myosin VI motor-coated quantum dots. 97% ± 1% (n = 123) of the myosin VI motor-coated quantum dots traveled from right to left, in the opposite direction as myosin V motor-coated quantum dots. This experiment further confirms that the polarized assay aligned the actin filaments well.

Thus far, we have discussed experiments with assays comprised of only one type of a motor, either myosin V or myosin VI. It is possible, however, to obtain simultaneous, bidirectional transport by concurrently introducing two types of motors, myosin V and myosin VI, into the flow cell. Myosin V and VI travel in opposite directions, and their concurrent engagement would be particularly interesting if each type of motor were to carry a different cargo. In our experiments, we labeled both myosin V and VI with the same type of quantum dot (QDs 655). Since the actin filaments in the polarized assay were well-oriented, we could differentiate myosin V motor-coated quantum dots from myosin VI motor-coated quantum dots according to their direction of motion. When the solution contained a mixture of myosin VI motor-coated quantum dots and myosin V motor-coated quantum dots in the ratio of 20:1, 41% ± 1% (n = 167) of the motile quantum dots traveled toward the actin filaments' minus ends. When the solution contained myosin VI motor-coated quantum dots and myosin V motor-coated quantum dots in the ratio of 1:1, only 13% ± 1% (n = 450) of the moving quantum dots walked toward the filaments' minus ends. These differences between myosin V motor-coated quantum dots and myosin VI motor-coated quantum dots might be due to differences in the interaction kinetics of myosin V and myosin VI.[34,35]

When both myosin V motor-coated quantum dots and myosin VI motor-coated quantum dots coexisted in the solution, we observed a few instances (n = 26) in which myosin V motor-coated quantum dots and myosin VI motor-coated quantum dots traveled on a collision course apparently along the same track in opposite directions (Figure 4a). The

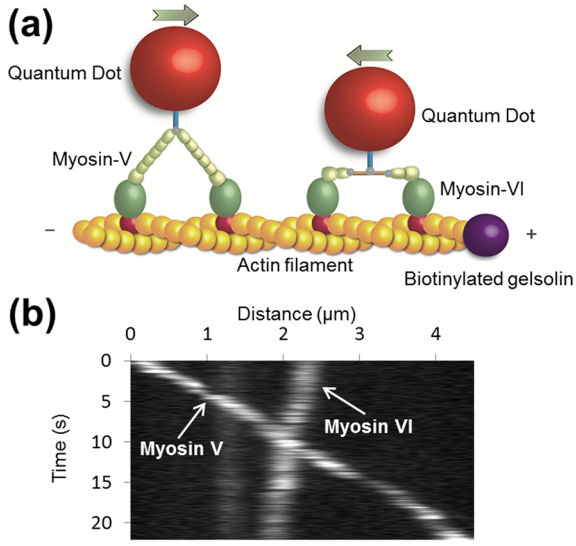

Figure 4. A schematic of a myosin V motor-coated quantum dot and myosin VI motor-coated quantum dot traveling on a "collision course" (a) and a time-space plot (kymograph) (b) of a typical myosin V motor-coated quantum dot and myosin VI motor-coated quantum dot passing event.

"collision event" resulted in one of the following outcomes: the two motor-coated quantum dots passing each other and continuing in their pre-encounter, opposite directions along the same track (65% of the n = 26 cases, Movie S3 of the Supporting Information, Figure 4b); the two motor-coated quantum dots stayed "frozen" (4% of the n = 26 cases); the myosin V motor-coated quantum dot detached (8% of the n = 26 cases); the myosin VI motor-coated quantum dot detached (15% of the n = 26 cases); and both motor-coated quantum dots detached (8% of the n = 26 cases). Figure 4b shows (bright lines) time-space trajectories (kymographs) of a myosin V motor-coated quantum dot and a myosin VI motor-coated quantum dot traveling in opposite directions. The crossing of the bright lines indicates a passing event.

An intriguing question is whether passing events can take place while the motors are traveling along a single filament. To this end, we needed to determine which tracks consist of a single filament and which of multiple filaments. Due to limitations of light microscopy, one cannot use direct observation to determine the number of filaments in the track. Instead, to make this determination, we rely on fluorescent emission intensity, arguing that the emission intensity is proportional to the number of filaments; that is, a track consisting of two parallel filaments will emit roughly twice the intensity of a single filament. Briefly, we illuminated the

dx.doi.org/10.1021/nl303500k | Nano Lett. 2013, 13, 79–84

surface with uniform intensity illumination by installing a reflecting, rotating mirror (at 1800 rpm) in the laser path.[36] The mirror reflects the incident laser light onto the surface evenly from all directions at angles that exceed the internal reflection angle. Images of actin filaments, the myosin V motor-coated quantum dots, and myosin VI motor-coated quantum dots were recorded with 100 ms exposure time at 5 frames per second. The emission intensities of both the actin filaments and the background were recorded with ImageJ software. The intensities' histogram (Figure S3 of the Supporting Information) formed a bimodal distribution with the peaks centered about intensities 1900 arbitrary units (A.U.) and 2 × 1900 A.U. No emission intensities lower than ∼1900 were observed. We associate intensity 1900 A.U. with that of a single filament and intensity 2 × 1900 A.U. with a two-filament bundle. In this way, we were able to identify tracks consisting of a single filament. A few of the passing encounters took place when the myosin V motor-coated quantum dot and the myosin VI motor-coated quantum dot were traveling along a single filament. This is the first report that two motors traveling in opposite directions along a *single* track can pass each other.

A technique, dubbed polarized assay, to orient, align, and immobilize actin filaments has been developed and tested. In contrast to prior works, the filaments retained their direction once the aligning force (flow) has been removed. We demonstrated that in assays comprised either of myosin V or VI motors-coated quantum dots alone, almost all of the motor-coated quantum dots traveled in one direction. In the polarized assay, 95% ± 1% (n = 774) of the myosin V motor-coated quantum dots traveled in the direction of the barbed (plus) end (against the direction of the flattening flow). Likewise, 97% ± 1% (n = 123) of the myosin VI motor-coated quantum dots traveled toward the pointed end (with the direction of the aligning flow). In contrast, the motion of myosin V motor-coated quantum dots was not directed, and the motors traveled randomly either to the right or to the left in the nonpolarized assay. The myosin V cargo transport efficiency was 78% ± 6% in the polarized assay, but only 10% ± 12% in the nonpolarized assay. The speed, run length, and run frequency were slightly less in the polarized assay than that in the nonpolarized assay. Longer run lengths and higher speeds could potentially be obtained by modifying the electrical charge of the myosin's binding site (loop 2) to actin,[37] using myosin V mutants with extended necks (containing more than the normal six calmodulin binding IQ motifs),[38] increasing the number of motors attached to each cargo,[39] and using higher ATP concentrations.[40] Simultaneous bidirectional cargo (quantum dot) transport was achieved by engaging both myosin V and myosin VI motors that "walk", respectively, toward the plus and minus ends of actin filaments. Myosin V motor-coated quantum dots and myosin VI motor-coated quantum dots were observed for the first time to pass each other while walking in opposite directions along a *single* actin filament. The technique presented here may be useful, among other things, for developing devices that utilize molecular motors as shuttles.

■ ASSOCIATED CONTENT

Supporting Information

Supplementary figures, movies, and detailed descriptions of the assays' preparations and experimental procedures. This material is available free of charge via the Internet at http://pubs.acs.org.

■ AUTHOR INFORMATION

Notes

The authors declare no competing financial interest.

■ ACKNOWLEDGMENTS

The work was supported, in part, by the National Science Foundation (NSF NSEC DMR08-32802) through the University of Pennsylvania's Nano-Bio Interface Center (NBIC). Dr. Mitsuo Ikebe (University of Massachusetts Medical School) generously gifted myosin V and myosin VI protein motors. Dr. Adam G. Hendricks assisted with TIRF microscopy. Mr. Matthew A. Caporizzo stimulated useful discussions.

■ REFERENCES

(1) Elowitz, M.; Lim, W. A. *Nature* **2010**, *468*, 889−890.
(2) Goel, A.; Vogel, V. *Nat. Nanotechnol.* **2008**, *3*, 465−475.
(3) Korten, T.; Månsson, A.; Diez, S. *Curr. Opin. Biotechnol.* **2010**, *21*, 477−488.
(4) Hess, H. *Annu. Rev. Biomed. Eng.* **2011**, *13*, 429−450.
(5) Holzbaur, E. L.; Goldman, Y. E. *Curr. Opin. Cell Biol.* **2010**, *22*, 4−13.
(6) van den Heuvel, M. G. L.; Dekker, C. *Science* **2007**, *317*, 333−336.
(7) Hess, H.; Clemmens, J.; Qin, D.; Howard, J.; Vogel, V. *Nano Lett.* **2001**, *1*, 235−239.
(8) Moorjani, S. G.; Jia, L.; Jackson, T. N.; Hancock, W. O. *Nano Lett.* **2003**, *3*, 633−637.
(9) Hess, H.; Matzke, C. M.; Doot, R. K.; Clemmens, J.; Bachand, G. D.; Bunker, B. C.; Vogel, V. *Nano Lett.* **2003**, *3*, 1651−1655.
(10) Clemmens, J.; Hess, H.; Howard, J.; Vogel, V. *Langmuir* **2003**, *19*, 1738−1744.
(11) Clemmens, J.; Hess, H.; Doot, R.; Matzke, C. M.; Bachand, G. D.; Vogel, V. *Lab Chip* **2004**, *4*, 83−86.
(12) van den Heuvel, M. G. L.; Butcher, C. T.; Smeets, R. M. M.; Diez, S.; Dekker, C. *Nano Lett.* **2005**, *5* (6), 1117−1122.
(13) Lin, C. T.; Kao, M. T.; Kurabayashi, K.; Meyhofer, E. *Nano Lett.* **2008**, *8*, 1041−1046.
(14) Dennis, J. R.; Howard, J.; Vogel, V. *Nanotechnology* **1999**, *10*, 232−236.
(15) Clemmens, J.; Hess, H.; Lipscomb, R.; Hanein, Y.; Bohringer, K. F.; Matzke, C. M.; Bachand, G. D.; Bunker, B. C.; Vogel, V. *Langmuir* **2003**, *19*, 10967−10974.
(16) Doot, R. K.; Hess, H.; Vogel, V. *Soft Matter* **2007**, *3*, 349−356.
(17) Riveline, D.; Ott, A.; Jülicher, F.; Winkelmann, D. A.; Cardoso, O.; Lacapère, J.-J.; Magnúsdóttir, S.; Viovy, J.-L.; Gorre-Talini, L.; Prost, J. *Eur. Biophys. J.* **1998**, *27*, 403−408.
(18) van den Heuvel, M. G. L.; Graaff, M. P.; Dekker, C. *Science* **2006**, *312*, 910−914.
(19) Kim, T.; Kao, M.-T.; Hasselbrink, E. F.; Meyhofer, E. *Nano Lett.* **2007**, *7*, 211−217.
(20) Kim, T.; Kao, M.-T.; Meyhofer, E.; Hasselbrink, E. F. *Nanotechnology* **2007**, *18*, 025101.
(21) Yokokawa, R.; Takeuchi, S.; Kon, T.; Nishiura, M.; Sutoh, K.; Fujita, H. *Nano Lett.* **2004**, *4*, 2265−2270.
(22) Yokokawa, R.; Yoshida, Y.; Takeuchi, S.; Kon, T.; Fujita, H. *Nanotechnology* **2006**, *17*, 289−294.
(23) Yokokawa, R.; Murakami, T.; Sugie, T.; Kon, T. *Nanotechnology* **2008**, *19*, 125505.
(24) Yokokawa, R.; Tarhan, M. C.; Kon, T.; Fujita, H. *Biotechnol. Bioeng.* **2008**, *101*, 1−8.
(25) Limberis, L.; Magda, J. J.; Stewart, R. J. *Nano Lett.* **2001**, *1*, 277−280.
(26) Brown, T. B.; Hancock, W. O. *Nano Lett.* **2002**, *2*, 1131−1135.
(27) Huang, L.; Manandhar, P.; Byun, K.-E.; Chase, P. B.; Hong, S. *Langmuir* **2006**, *22*, 8635−8638.

(28) Spudich, J. A.; Kron, S. J.; Sheetz, M. P. *Nature* **1985**, *315*, 584−586.
(29) Wei, M-Y; Leon, L. J.; Lee, Y.; Parks, D.; Carroll, L.; Famouri, P. *J. Colloid Interface Sci.* **2011**, *356*, 182−189.
(30) Yin, H. L.; Stossel, T. P. *Nature* **1979**, *281*, 583−586.
(31) Ashman, K. M.; Bird, C. M.; Zepf, S. E. *Astron. J.* **1994**, *108*, 2348−2361.
(32) Ruhnow, F.; Zwicker, D.; Diez, S. *Biophys. J.* **2011**, *100*, 2820−2828.
(33) Kakugo, A.; Shikinaka, K.; Matsumoto, K.; Gong, J. P.; Osada, Y. *Bioconjugate Chem.* **2003**, *14*, 1185−1190.
(34) De La Cruz, E. M.; Wells, A. L.; Rosenfeld, S. S.; Ostap, E. M.; Sweeney, H. L. *Proc. Natl. Acad. Sci. U.S.A.* **1999**, *96*, 13726−13731.
(35) De La Cruz, E. M.; Ostap, E. M.; Sweeney, H. L. *J. Biol. Chem.* **2001**, *276*, 32373−32381.
(36) Mattheyses, A. L.; Shaw, K.; Axelrod, D. *Microsc. Res. Technique* **2006**, *69*, 642−647.
(37) Hodges, A. R.; Krementsova, E. B.; Trybus, K. M. *J. Biol. Chem.* **2007**, *282*, 27192−27197.
(38) Sakamoto, T.; Yildiz, A.; Selvin, P. R.; Sellers, J. R. *Biochemistry* **2005**, *44*, 16203−16210.
(39) Lu, H.; Efremov, A. K.; Bookwalter, C. S.; Krementsova, E. B.; Driver, J. W.; Trybus, K. M.; Diehl, M. R. *J. Biol. Chem.* **2012**, DOI: jbc.M112.371393.
(40) Forkey, J. N.; Quinlan, M. E.; Shaw, M. A.; Corrie, J. E. T.; Goldman, Y. E. *Nature* **2003**, *422*, 399−404.